NMR chemical shifts of ice and liquid water: the effects of condensation.

Bernd G. Pfrommer[a], Francesco Mauri[b], and *Steven G. Louie[a]
[a] *Department of Physics, University of California at Berkeley, Berkeley, CA 94720, USA, and Materials Sciences Division, Lawrence Berkeley National Laboratory, Berkeley, CA 94720, USA.*
[b] *Laboratoire de Minéralogie-Cristallographie de Paris, (Universités P6 et P7, CNRS), case 115, 4 place Jussieu, 75252 Paris, France*
(April 15, 2000)

We report the results of ab initio density functional theory calculations of the NMR chemical shift of liquid water and hexagonal ice. Depending on the structural model used, the calculated isotropic shift of ice Ih with respect to the gas phase is -8.0 ± 0.2ppm or -8.1 ± 0.1ppm for the proton, and -48.6 ± 0.02ppm or -48.1 ± 0.02ppm for oxygen. The proton anisotropy is -33.4 ± 0.2ppm or -33.6 ± 0.2ppm. Using snapshots from ab initio molecular dynamics simulations, we find a gas-to-liquid shift of -5.8 ± 0.1ppm for hydrogen, and -36.6 ± 0.5ppm for oxygen. Molecules beyond the first solvation shell influence the proton chemical shift predominantly via the electric field generated by their permanent electric dipole moment. Finally, we show that it is possible to reproduce the proton chemical shifts in the condensed phases by an empirical function of the local molecular geometry.

I. INTRODUCTION

NMR chemical shift measurements in aqueous solutions are a highly popular analysis technique in chemistry. One of the more common solvents is water, and it is well known that hydrogen bonds play an important role for the condensed phases of water[1–3]. However, the influence of the hydration on the chemical shift of a solute is still not fully understood on a microscopic level. This has motivated us to calculate the gas-to-liquid proton and oxygen shifts of water, where water is both the solvent and the solute. We also report calculations for another condensed phase of water, hexagonal ice Ih, where the location of the hydrogen atoms is not well established[4], and conflicting experimental values for the proton chemical shift are reported in the literature[5–8]. Our results, combined with more accurate experiments, could be used to indirectly determine the average OH bond length of ice Ih.

With regards to solvent effects on proton chemical shifts in liquid water, two main thrusts can be identified in the literature. One aims at advancing the computational methods to accurately reproduce the experimentally observed gas-to-liquid shift[9–17]. The other is more concerned with explaining the physics behind the shift, and in particular the role of electric field effects[15,18–20]. Our study ties these two areas together, and advances the understanding on both frontiers.

Unlike previous calculations[9–14], our ab initio density functional theory (DFT) approach[21] does not model solid and liquid water with finite clusters, but treats them as infinite, periodic systems. To our knowledge, the present work is also the first study employing molecular geometries generated by true ab initio Car-Parrinello molecular dynamics simulations[22]. Since we are using an infinite system to model the condensed phases, our results do not suffer from finite size limitations.

II. NUMERICAL METHOD AND TECHNICAL DETAILS

A uniform, external magnetic field $\mathbf{B}_{\rm ext}$ applied to a spherical sample of matter induces an electronic current which produces a non-uniform magnetic field, $\mathbf{B}_{\rm in}(\mathbf{r})$. The chemical shielding tensor $\overleftrightarrow{\sigma}$ relates the induced magnetic field to the applied magnetic field:

$$\mathbf{B}_{\rm in}(\mathbf{r}) = -\overleftrightarrow{\sigma}(\mathbf{r})\mathbf{B}_{\rm ext} \ . \tag{1}$$

This magnetic response is a fingerprint of the sample's microscopic structure. NMR measures $\overleftrightarrow{\sigma}(\mathbf{r})$ at the nuclear positions. Often, experiments only measure the isotropic shielding $\sigma(\mathbf{r}) = \mathrm{Tr}(\overleftrightarrow{\sigma}(\mathbf{r}))/3$. We further define the anisotropy to be $\Delta\sigma = \sigma_{11}^{(s)} - (\sigma_{22}^{(s)} + \sigma_{33}^{(s)})/2$, assuming the principal values $\sigma_{11}^{(s)}, \sigma_{22}^{(s)}, \sigma_{33}^{(s)}$ of the symmetrized tensor $\overleftrightarrow{\sigma}^{(s)} = (\overleftrightarrow{\sigma} + \overleftrightarrow{\sigma}^T)/2$ to be ordered such that $\sigma_{11}^{(s)} > \sigma_{22}^{(s)} > \sigma_{33}^{(s)}$. With σ(H), we denote the shielding at the hydrogen nuclei, and with σ(O) the shielding at the oxygen nuclei.

We compute $\overleftrightarrow{\sigma}$ following Ref. 21. The electronic structure is described using density functional theory (DFT) in the local density approximation (LDA). As long as the geometry is kept the same, and only *relative* chemical shifts

are considered, the results are quite insensitive to the functional used. For example, our test calculations show that the gas-to-ice isotropic proton shifts obtained using the PW91 generalized gradient approximation (GGA) differ by less than 0.15ppm from the corresponding LDA results. As the core contributions for oxygen are insensitive to the chemical environment[23], we consider the magnetic response of the valence electrons only. We use norm-conserving pseudopotentials[24] in the Kleinman-Bylander form[25]. For H, a purely local pseudopotential is used, whereas for O, a non-local s-projector augments the local potential. The Kohn-Sham orbitals are expanded in plane waves up to an energy cut-off of 70 Ry.

We will quote chemical shifts δ with respect to the shift of an isolated reference molecule,

$$\delta(X) = \sigma(X) - \sigma_{\rm ref}(X), \qquad X = \mathrm{H}, \mathrm{O}, \tag{2}$$

where $\sigma(X)$ is measured for a sample of spherical shape. A subscript to σ and δ will be used to indicate the phase of the sample. For the geometry of the reference molecule, we use an equilibrium radius and angle of $r_{\rm e} = 0.968$Å and $\angle$HOH$= 104.2^o$, respectively, which have been computed[26,27] using DFT/GGA with the Perdew-Burke-Ernzerhof (PBE) functional[28]. We use the GGA-relaxed geometry in order to be consistent with the geometry for the ice and water simulations, which have also been computed using GGA[29]. Due to the frozen core approximation, we cannot compute absolute shieldings for oxygen. For hydrogen, however, this is possible, since it has no core electrons. Our calculated shielding of $\sigma_{\rm ref}$(H) = 30.1ppm, and anisotropy of $\Delta\sigma_{\rm ref}$(H) = 20.4ppm, are in good agreement with the Hartree-Fock results from Ref. 30, where 30.9ppm and 19.7ppm, respectively, are reported. In experiment, an isotropic shielding of 30.05±0.015 ppm is measured[31], but the excellent agreement with theory could be fortuitous, since the experimental number includes rovibrational effects, as discussed below[32].

The value of $\sigma_{\rm ref}$ for a rigid molecule at the equilibrium geometry differs from the gas phase due to neglected rovibrational corrections. A realistic calculation of the gas phase shielding requires a MD simulation at low densities, and a statistical averaging of $\sigma_{\rm gas}$. This "classical" correction is small[33], but does not include the effect of the quantum-mechanical zero-point motion of the hydrogen. For an isolated molecule, Vaara et al.[34] calculated that the zero-point motion shifts $\sigma_{\rm e}$(H) by -0.52ppm, and $\sigma_{\rm e}$(O) by -11.7ppm. Hopefully, the effect is similar in gas, liquid, and ice, and therefore cancels out when relative shifts are considered, as it is done in the present work[35].

III. HEXAGONAL ICE

Depending on pressure and temperature, ice can assume many different crystal structures[36,37]. In this work, we focus on the most common form, hexagonal ice Ih, which forms at ambient pressure[38]. Hexagonal ice is a crystal with static and/or dynamic disorder, i.e. although the atomic configurations differ from one unit cell to the other, the time and space *averaged* coordinates are highly symmetric. On the average, the oxygen atoms in ice Ih are arranged on a hexagonal lattice, such that each oxygen has four neighboring oxygens in a tetragonal configuration. While the oxygen lattice is easily resolved in X-ray or neutron scattering spectroscopy, the average position of the hydrogen atoms is uncertain[4].

In our simulations, we are restricted to a static, periodic model of ice which we design to resemble the disordered phase. We use supercells in which we place the oxygen atoms exactly at their symmetric, averaged lattice sites, and the hydrogen atoms at arbitrary sites following the "ice rules"[1]. To verify the validity of this approach, we have used two different models: model A, as shown in Fig. 1, with four molecules in the primitive unit cell, and model B, which is the Bernal model proposed in Ref. 26, with 12 molecules in the primitive unit cell.

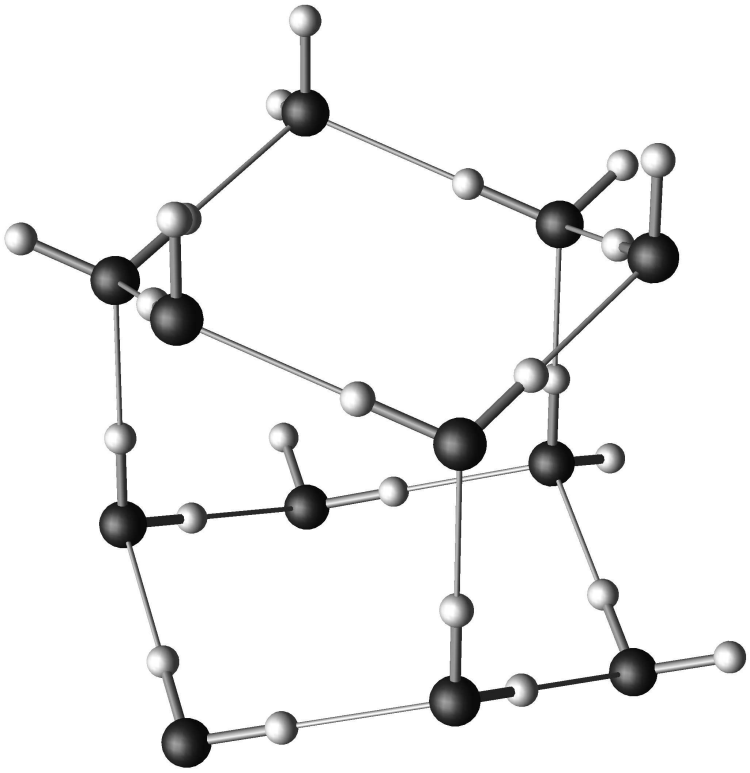

FIG. 1. Ordered model A of hexagonal ice Ih, with four molecules in the primitive unit cell. Oxygen atoms are shown dark, hydrogen atoms are rendered light grey. The hydrogen bonds are drawn as thin, grey lines for ease of visualization.

For simplicity, the hydrogen atoms are placed on straight lines between neighboring oxygen atoms, which results in a bond angle of $\angle$HOH= 109.47^o. In test calculations, we relaxed the restriction on both the oxygen and hydrogen positions, but there was only a negligible effect on the chemical shift. For both models, the OH bond length is set to the average GGA(PBE)-relaxed value of 0.993Å reported for model B[26,27]. We employ the experimental lattice parameters[38] of $a = 4.50$Å, and $c = 7.32$Å at $T = 0K$, which for practical purposes are identical to the GGA(PBE)-relaxed values[26].

Both models yield very similar results for the gas-to-ice shift, as shown in Table 1. Since not all atoms of a kind are crystallographically equivalent, the maximum fluctuation of $\delta_{\rm ice}(X)$ and $\Delta\sigma_{\rm ice}(X)$ is indicated by the error bars in Table 1.

sample	T[K]	$\delta_{\rm ice}$(H)	$\Delta\sigma_{\rm ice}$(H)	$\delta_{\rm ice}$(O)	Ref.
H_2O model A	0	-8.0 ± 0.1^a	33.4 ± 0.2	-48.6 ± 0.02^a	this work
H_2O model B	0	-8.1 ± 0.1^a	33.6 ± 0.2	-48.1 ± 0.02^a	this work
H_2O polycrystalline	77	-9.7 ± 1.0^b	28.7 ± 2.0	-	Exp. Ref. 5
H_2O single crystal	77	-7.4^b	28.5	-	Exp. Ref. 6
D_2O polycrystalline	183	-2.4 ± 2.0^b	34 ± 4	-	Exp. Ref. 7
H_2O polycrystalline	173	0.4 ± 0.7^b	34.2 ± 1.0	-	Exp. Ref. 8

TABLE 1. Measured and computed isotropic chemical shifts $\delta_{\rm ice}$(H), $\delta_{\rm ice}$(O), and anisotropies $\Delta\sigma_{\rm ice}$(H), in parts per million (ppm) for hexagonal ice Ih. The reference point for calculated shifts is an isolated molecule with a rigid GGA(PBE)-relaxed geometry. Note that the $T = 0$K geometry for ice does not include zero point vibrations.
[a]The error bar represents the variations between crystallographically non-equivalent atoms of the same kind.
[b]Computed from the quoted liquid-to-ice shifts, and assuming a gas-to-liquid shift of -4.34ppm from Ref. 39.

Due to the lack of long range order, ice Ih is not ferroelectric, i.e. the dipole moment per molecule averaged over a macroscopic sample is zero. Because our approach imposes an artificial periodicity, our models possess a non-vanishing net electric dipole moment, and are therefore ferroelectric. Using a simplified electrostatic point charge approach, we estimate the net dipole moment to be 0.91 (model A) and 0.58 (model B) per molecule, in units of the average molecular dipole. Despite the difference, the calculated chemical shifts of the two models are very similar, from which we conclude that the ice shifts are not affected by the ferroelectricity of the models.

Comparison with experiment is difficult, since the available data date back to the late seventies, and are not sufficiently accurate. We could only find hydrogen shift measurements published for ice, but no experiments on the oxygen shift. Moreover, the experimental proton shifts published by different groups appears to be conflicting. As far as $\delta_{\rm ice}$(H) is concerned, our calculations support the measurements of Ref. 5 and 6, albeit there is some deviation from the polycrystalline data. We are in clear disagreement with $\delta_{\rm ice}$(H) reported in Ref. 7 and Ref. 8. Although the latter experiments have been performed at different temperatures, we cannot think of a mechanism that would lead to such a strong temperature dependence of $\delta_{\rm ice}$(H). The fact that the well established gas to liquid shift at room temperature is already about -4.4ppm (cf Table 2), and actually increases in magnitude with decreasing temperature, is further in support of the results reported in Refs. 5 and 6.

In view of these facts, we believe the isotropic proton shifts reported in Refs. 7, 8 are incorrect. According to one of the authors of Ref. 7, their experiment was more geared towards an accurate measurement of the anisotropy[40], with which our calculated values agree nicely. The small discrepancy between our computed anisotropy, and the measured values reported in Refs. 5 and 6 remains unexplained.

As mentioned earlier, the average OH bond length of ice Ih is not known with certainty. Diffraction studies[41,42] on H_2O and D_2O indicate an average bond length of 1.01Å, but compared to the bond length of other polymorphs of ice, this seems too long[4]. In Fig. 2, we show the calculated $\Delta\sigma_{\rm ice}$(H) (upper panel) and $\delta_{\rm ice}$(H) (lower panel) as a function of OH bond length. Between 0.95 and 1.00 Å, both are linearly dependent on the bond length, with slopes of -7.0 and -26.4 ppm/Å, respectively. Thus, the isotropic shift is more sensitive to the OH bond length, and better suited to indirectly determine the average bond length of ice Ih. In Fig. 2, we indicate with dashed lines the experimental results from Refs. 5 and 6 for a single crystal and a polycrystalline sample. Although the experimental resolution is insufficient to deduce the OH bond length, we believe that these experiments could nowadays be repeated with higher accuracy. Combining experiment with our calculated results might then allow to bracket the average bond length in ice Ih.

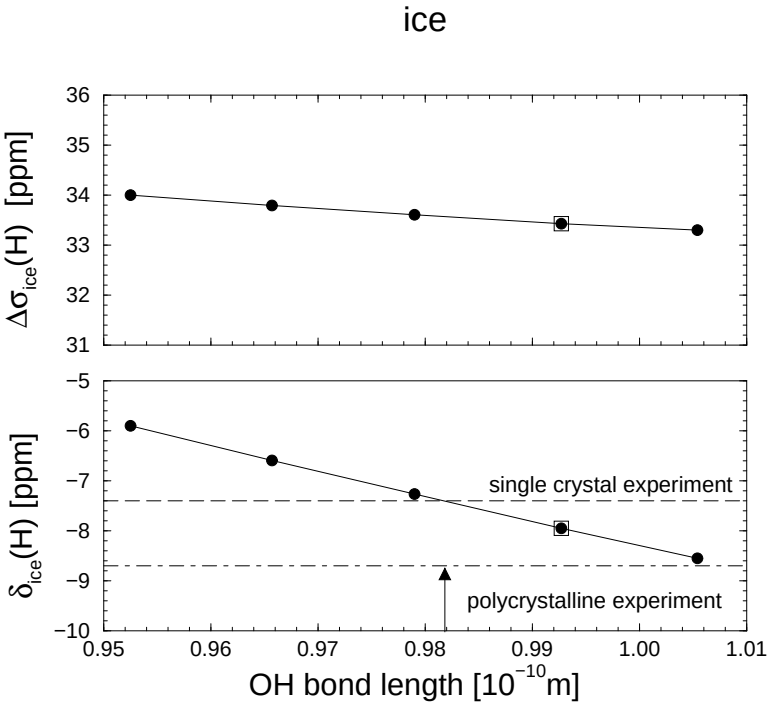

FIG. 2. Computed NMR chemical shift (in ppm) of hydrogen in ice Ih (model A) as a function of the OH bond length (in Å). The lower panel shows the isotropic shift $\delta_{\rm ice}$(H) with respect to an isolated water molecule. The dashed horizontal line represent single-crystal experimental results from Ref. 6, the dot-dashed horizontal line is the upper limit (denoted by an arrow) of the polycrystalline experiments from Ref. 5. In the upper panel, the anisotropy $\Delta\sigma_{\rm ice}$(H) is plotted. The data points at the average GGA-relaxed OH bond length are marked with open squares. Notice that upper and lower panel are plotted on the same scale.

IV. LIQUID WATER

To model liquid water, we obtained nine snapshots from an ab initio molecular dynamics (MD) simulation by Sprik et al[3], which was done at a density of 1.00 g/cm^3 and at a temperature of 300K, using state-of-the-art Car-Parrinello[43] MD techniques, based on DFT/GGA. The Becke-Lee-Yang-Parr (BLYP) functional was used, since it gave the best description of the hydrogen bond[3]. A cubical supercell with 32 water molecules inside, and an edge length of 9.865Å is periodically replicated. Due to the finite number of snapshots, there is a statistical uncertainty in the averaging procedure, which we indicate with an error bar ($\pm$). It is computed by dividing the standard deviation of the chemical shift by $\sqrt{n}$, where n is the number of atoms in all simulation snapshots, $n = 576$ for hydrogen, and $n = 288$ for oxygen.

To get a better understanding of the gas-to-liquid shift, we will now compute the average chemical shift for progressively larger clusters of water molecules. First, we isolate all 288 molecules from the MD snapshots, and compute their shifts δ_1. After that, all possible 576 dimers are selected, and the shifts δ_2(H) of the hydrogen-bonding protons are computed. Next, we pick 288 pentamers, and compute the shifts δ_5 of the central water molecules, which are now surrounded by a complete first solvation shell. Finally, we compute the full liquid shifts δ for the entire simulation cell. The so-obtained averaged shifts are listed in Table 2. Also shown there are results by Malkin et al[12], which have been computed with a DFT sum-over-states (SOS) approach[44], and are based on molecular geometries generated by force field MD simulations with a Lie and Clementi[45] interaction potential.

symbol	sample	T[K]	H	O
		THEORY, PRESENT STUDY		
δ_1	H_2O	300	-0.94 ± 0.03	-7.5 ± 0.4
δ_2	$(H_2O)_2$	300	-3.64 ± 0.08	-12.6 ± 0.3
δ_5	$(H_2O)_5$	300	-4.95 ± 0.09	-33.0 ± 0.6
$\delta_{\rm liq}$	liquid	300	-5.83 ± 0.10	-36.6 ± 0.5
		THEORY, REF. 12		
-	H_2O	300	-0.33 ± 0.07	-6.0 ± 1.4
-	$(H_2O)_5$	300	-2.94 ± 0.44	-31.0 ± 2.4
-	$(H_2O)_7$	300	-3.03 ± 0.22	-36.4 ± 2.1
-	$(H_2O)_{13}$	300	-3.22 ± 0.20	-37.6 ± 2.1
		EXPERIMENT		
$\delta_{\rm liq}$	liquid	273	-4.66^a	-
$\delta_{\rm liq}$	liquid	300	-4.34^b	-36.1^c
$\delta_{\rm liq}$	liquid	350	-3.77^a	-

TABLE 2. Computed chemical shifts δ(H) and δ(O) of hydrogen and oxygen, repectively, for water n-mers (n = 1,2,5,9,13), and for the full liquid. All values are given in parts per million (ppm). Calculated shifts are quoted with respect to an isolated, rigid, GGA(PBE)-relaxed reference molecule. For comparison, experimental data from ^{a}Ref. 39, and ^{c}Ref. 46, interpolated experimental results from ^{b}Ref. 47, and theoretical results from Ref. 12 are presented.

Evidently, the shift δ_1 is due to the deformation of the water molecules in the liquid phase, for example a stretching of the average OH bond length by 0.024 Å. Notice the strong effect of the nearest neighbor molecule on the proton shift: δ_2(H) is already more than half of the total liquid shift, $\delta_{\rm liq}$(H). However, even the pentamer proton shift δ_5(H) is still off by 0.9ppm from the full liquid shift, $\delta_{\rm liq}$(H). Considering the larger absolute shift, that same relative difference is smaller for oxygen. For the full liquid simulation, we find an average gas-to-liquid shift of $\delta_{\rm liq}({\rm H}) = -5.83 \pm 0.10$ppm, and $\delta_{\rm liq}({\rm O}) = -36.6 \pm 0.5$ppm. The oxygen shift is close to the experimental one of -36.1ppm. However, we overestimate the magnitude of the hydrogen shift by about 1.5 ppm compared to experiment.

Part of our overestimation of $\delta_{\rm liq}$(H) could come from neglecting the difference in rovibrational effects between gas and liquid phase, as mentioned earlier. More likely however, the error is due to an inaccurate geometry of the water molecules taken from the MD snapshots. Ref. 12 reports a variation of up to 0.6ppm for the average hydrogen gas-to-liquid shift, depending on which force field is used. Considering the strong dependency of $\delta_{\rm liq}$(H) on the temperature (cf Table 2), and furthermore the fact that the DFT/GGA errors[3] in the hydrogen bonding energy can be of the order of $k_{\rm B}T$, with $T = 300$K, the agreement with experiment is quite good. Notice that although the MD simulations using the BLYP functional in Ref. 3 give the best description of the hydrogen bond, both the diffusion coefficient and the relaxation time suggest that the hydrogen bonding is too strong. This is in line with our overestimation of $\delta_{\rm liq}$(H), since a stronger hydrogen bond will bias the calculation towards larger $\delta_{\rm liq}$(H). Furthermore, the basis set used for the liquid MD simulations is not quite sufficient, and has been shown in Ref. 3 to lead to a .004Å increase in bond length for an isolated molecule. Assuming that the resulting change in the shielding is identical for an isolated molecule and for the liquid, our gas-to-liquid shifts would change to $\delta_{\rm liq}({\rm H}) = -5.64 \pm 0.1$ppm and $\delta_{\rm liq}({\rm O}) = -35.1 \pm 0.5$ppm. We do not expect the inaccuracies of LDA in the computation of σ for a given geometry to be a major source of error, since the inclusion of correlation effects changes the hydrogen shift of the water molecule by only 0.2ppm from the "uncorrelated" Hartree-Fock value[48,49]. It is not sure whether this is still a valid assumption also when hydrogen bonds are present. However, as outlined in Section II, our test calculations show very little difference between relative GGA and LDA shifts, indicating that deficiencies in the LDA correlation terms, and the overestimation of the hydrogen bond strength in LDA, are a not a source of significant error.

We will now compare our results with earlier calculations found in the literature. As shown in Table 2, Ref. 12 reports a significantly smaller δ_1(H) due to the molecular gas-to-liquid distortion. This could indicate substantial differences in the molecular geometries generated by the MD simulations in Ref. 12, and the ones that we employ. That would also explain the discrepancies for δ_5(H), but would further imply that the oxygen shifts, which are in fairly good agreement (see Table 2), are less sensitive to the geometry. The previously published dimer hydrogen shifts of -2.95ppm[9], -2.8ppm[11], and -2.81ppm[10,13] have been calculated with different dimer geometries, and therefore cannot be directly compared with our results. In contrast to our calculation, earlier work based on finite water clusters tends to *underestimate* the magnitude of the proton gas-to-liquid shift. Chesnut and Rusiloski[14] for instance report a shift of only $\delta_{10}({\rm H}) = -2.28$ppm, using five clusters consisting of 10 molecules, and a Hartree-Fock gauge including atomic orbitals (GIAO) method. Malkin et al[12] compute an average $\delta_{\rm liq}$(H) between -2.8ppm and -3.4ppm, depending on the force field used. They use clusters of up to 13 molecules, where, according to their convergence tests, the shift should be approaching the limit of a liquid to within fractions of a ppm. Since our overestimation of $\delta_{\rm liq}$(H) is comparable to their underestimation of it, it is not clear whether ab initio MD using the GGA BLYP functional yields molecular coordinates that, for the purpose of shift calculations, are superior to those generated by force field methods. Finally, by using a classical dielectric model and a single water pentamer, Mikkelsen et al[15] calculate $\delta_{\rm liq}({\rm H}) = -3.97$ppm.

V. ROLE OF THE ELECTRIC FIELD

What is the physics behind the hydrogen gas-to-liquid shift? It is unlikely that quantum-mechanical effects would extend much beyond the first hydration shell. On the other hand, water molecules possess a permanent electric dipole moment, and the corresponding electric field is of long range. Thus, there is hope that the influence of molecules beyond the first hydration shell can be reduced to the electric field they generate at the position of the proton. Several published studies exploit this idea[20,39,47], but they are not based on ab initio calculations, and are restricted to the *average* shift due to the *average* electric field on the proton. We do not expect such an approach to accurately reproduce the shift of *individual* protons. The hydrogen bond is short enough for genuine quantum-mechanical effects to play a role[9]. In this section, we will look at the shifts of individual protons, and how they are related to the electric field. Our study parallels earlier work on protein molecules[18,19], where the proton shift is also affected by electrostatics.

We start out by labeling the protons of the MD snapshots with an index $i = 1, ..N_{\rm H}$, $N_{\rm H} = 576$, and denoting their shift with $\delta({\rm H}_i)$. To quantify the aberration of dimer shifts $\delta_2({\rm H}_i)$ and pentamer shifts $\delta_5({\rm H}_i)$ from the liquid shifts

$\delta_{\rm liq}({\rm H}_i)$, we further introduce

$$\rho_n = \left(\frac{1}{N_{\rm H}} \sum_{i=1}^{N_{\rm H}} (\delta_n({\rm H}_i) - \delta_{\rm liq}({\rm H}_i))^2 \right)^{1/2}, \qquad n = 2, 5 \ . \tag{3}$$

Now, we correct the dimer and pentamer shifts by an amount that is proportional to the difference in electric field $\Delta E_n({\rm H}_i)$, calculated at the position of proton i by using the ab initio electron densities, and projected onto the normal vector $\hat{\mathbf{b}}_i$ pointing along the OH bond, directed from O to ${\rm H}_i$:

$$\delta_n^{(\rm corr)}({\rm H}_i) = \delta_n({\rm H}_i) + A_n \Delta E_n({\rm H}_i) \qquad i = 1, ..N_{\rm H}, \qquad n = 2, 5, \tag{4}$$

$$\Delta E_n({\rm H}_i) = (\mathbf{E}_{\rm liq}({\rm H}_i) - \mathbf{E}_n({\rm H}_i)) \cdot \hat{\mathbf{b}}_i \ . \tag{5}$$

If the electric field difference is indeed responsible for the difference in shift, then a properly chosen constant A_n will bring the corrected shifts close to the liquid ones. We determine A_n by a least-squares fit to the liquid shifts, i.e. by minimizing the aberration

$$\rho_n^{(\rm corr)} = \left(\frac{1}{N_{\rm H}} \sum_{i=1}^{N_{\rm H}} (\delta_n^{(\rm corr)}({\rm H}_i) - \delta_{\rm liq}({\rm H}_i))^2 \right)^{1/2} . \tag{6}$$

We neglect the electric field components perpendicular to the bond, since on the average, they are smaller than the parallel component by more than an order of magnitude, and σ(H) is most susceptible to electric fields parallel to the bond. We further neglect hyper- and quadrupole shielding polarizabilities, since we already include the dominant electric field effects of the nearest-neighbor molecule to all orders. We quote the electric field in atomic units (a.u.) following the Hartree convention, where 1a.u.$= 5.14 \times 10^9$V/m.

Fig. 3 shows the dimer shifts of $N_{\rm H}$ hydrogen atoms (along the y axis), as a function of the corresponding full liquid shift (along the x axis). The grey, solid triangles are the bare $\delta_2({\rm H}_i)$ of the hydrogen-bonding proton. The black, open triangles represent $\delta_2^{(\rm corr)}({\rm H}_i)$, as defined in Eqs (4) and (5), with $A_2 = 151$ppm/a.u. The correction reduces the aberration from $\rho_2 = 2.7$ppm to $\rho_2^{(\rm corr)} = 0.83$ppm. The average electric field difference is $\Delta E_2({\rm H}) = 0.0138$a.u, and leads to an average $\delta_2^{(\rm corr)}({\rm H})$ of -5.73ppm, which is just 0.1 ppm off the computed liquid shift (-5.83ppm). Interestingly, even for the protons with a strong shift of $\delta_{\rm liq}({\rm H}_i) < -6$ppm, the *average* corrected dimer shift is in good agreement with the *average* liquid shift. However, the *individual* $\delta_2^{(\rm corr)}({\rm H}_i)$ can stray significantly off the ideal $x = y$ line, indicating that in this regime, the simple electric field correction is no longer accurate.

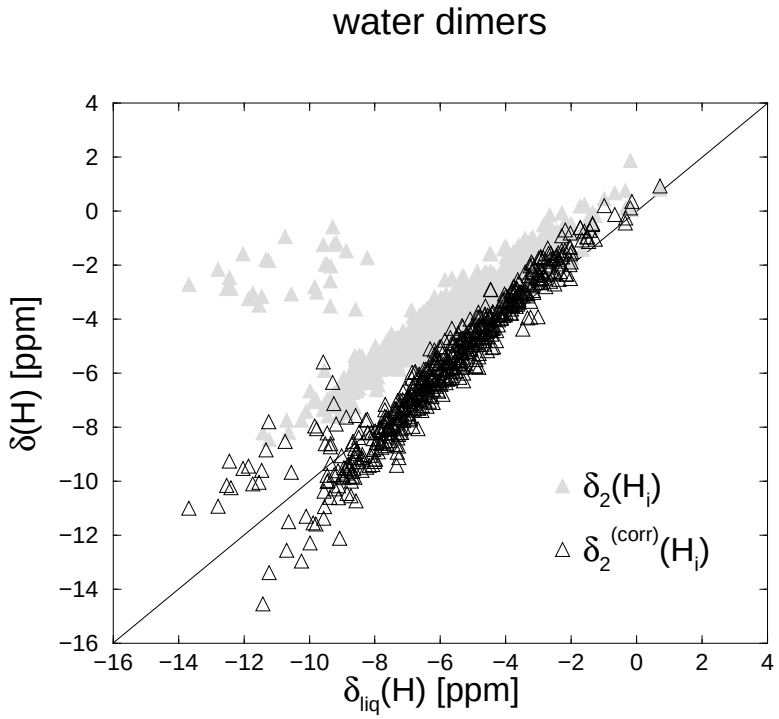

FIG. 3. Isotropic hydrogen chemical shifts of isolated water dimers. Each symbol corresponds to a hydrogen atom. Along the x-axis and y-axis, the full liquid shifts $\delta_{\rm liq}({\rm H}_i)$, and the shifts of a dimer configuration, respectively, are plotted. The grey, solid symbols show the bare $\delta_2({\rm H}_i)$ shifts. When correcting for electric field effects, the resulting $\delta_2^{(\rm corr)}({\rm H}_i)$ (shown as black, open symbols) are much closer to the liquid shifts, and hence to the $x = y$ line.

Repeating for water pentamers an analogous procedure as for the water dimers above, the results shown in Fig. 4 are obtained. As expected, the aberration $\rho_5 = 0.96$ppm for the bare pentamer shifts $\delta_5({\rm H}_i)$ (black, open squares) is smaller than the aberration $\rho_2 = 2.7$ppm for the dimers. When correcting for electric field effects, the aberration drops to $\rho_5^{(\rm corr)} = 0.33$ppm. The fitted proportionality constant is $A_5 = 101$ppm/a.u. In contrast to the dimers, the electric field correction for pentamers works quite well even for strong shifts. The largest error committed is $\max_i |\delta_5^{(\rm corr)}({\rm H}_i) - \delta_{\rm liq}({\rm H}_i)| = 1.3$ppm. Notice that both fitted constants, $A_2 = 151$ppm/a.u. and $A_5 = 101$ppm/a.u. are in general agreement with the shielding polarizability $A_1 = 89.6$ppm/a.u along the bond of an isolated water molecule, which we calculated from A_x and A_z published in Table IX of Ref.[50]. This is strong evidence that the electric field is indeed responsible for the observed behavior in the shift, and not some other physical effect related to the local structure. The discrepancy between A_2 and A_1 is most likely due to the fact that A_2 incorporates some non-electric short-range effects, more so than A_5.

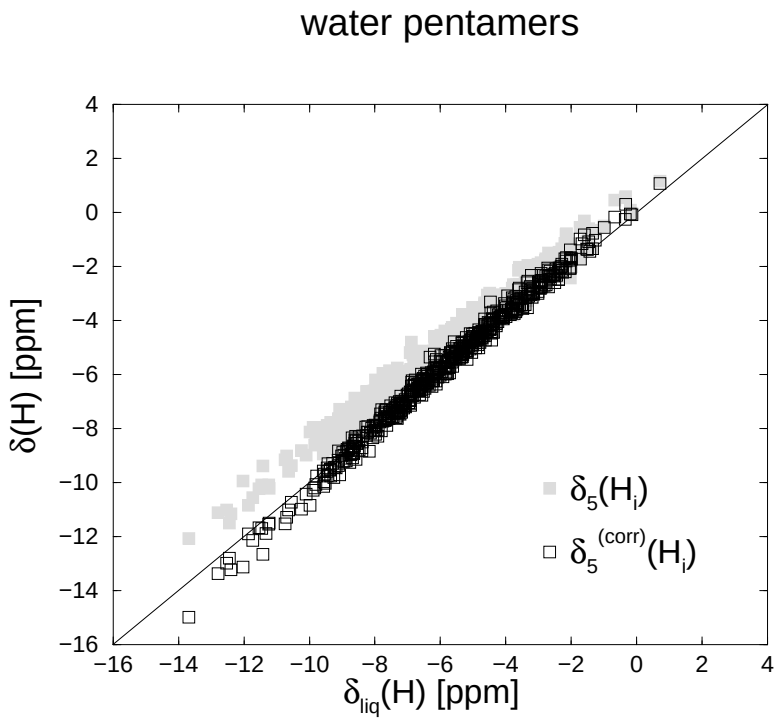

FIG. 4. Isotropic hydrogen chemical shifts of isolated water pentamers. Along the x-axis, the full liquid shift $\delta_{\rm liq}({\rm H}_i)$ is plotted. On the y-axis, the pentamer shifts $\delta_5({\rm H}_i)$ (grey, solid symbols) and $\delta_5^{(\rm corr)}({\rm H}_i)$ (black, open symbols) are shown.

Fig. 4 suggests that one can compute the chemical shift with fairly high accuracy by selecting pentamers from the MD simulation cell, and representing the molecules beyond the first hydration shell by the electric field that they generate at the hydrogen position, as given by Eqs. (4) and (5). Future quantum-chemistry calculations can take advantage of this fact. In the following section, we go one step further by demonstrating that $\delta_{\rm liq}({\rm H}_i)$ can be computed accurately based solely on geometrical considerations. This leads to a simple and useful formula to compute the hydrogen chemical shift in liquid water without any ab initio calculation required.

VI. ROLE OF THE GEOMETRY

The hydrogen gas to liquid shift depends crucially on the liquid geometry, as shown in Ref. 12. To study this structural effect, we parametrize $\delta_{\rm liq}({\rm H}_i)$ of each molecule of our liquid samples in terms of the geometry of the H_2O pentamer cluster, which, in the liquid, includes and surrounds the molecule, as shown in Fig. 5. We find a particularly strong correlation between $\delta_{\rm liq}({\rm H}_i)$ and the length of the OH_i covalent bond d_c, the molecular HOH_i angle α, the

length of the hydrogen bond (d_1), and the lengths of the secondary hydrogen bonds d_3 and d_4[51]. These geometrical parameters are depicted in Fig. (5). The function which we found to best fit the ab-initio results for the liquid is:

$$\delta_5^{(\mathrm{fit})}(\mathrm{H}_i) = 36.322 - 31.186\, d_c - \frac{31.712}{d_1^3} - \frac{4.596}{d_3^3} - \frac{4.596}{d_4^3} - 0.05052\,\alpha \tag{7}$$

where the lengths are computed in Å, the angles in degrees, and $\delta_5^{(\mathrm{fit})}(\mathrm{H}_i)$ is given in ppm. Notice that $\delta_5^{(\mathrm{fit})}(\mathrm{H}_i)$ is the shift of a pentamer *embedded in the liquid*, and is therefore different from the shift of the isolated pentamer. The aberration of this parametrization from the ab-initio liquid shifts is $\rho_5^{(\mathrm{fit})} = 0.43$ppm, which is competitive with the value of $\rho_5^{(\mathrm{corr})} = 0.33$ppm that we obtained earlier from corrected ab initio calculations on pentamers. A comparison between $\delta_5^{(\mathrm{fit})}(\mathrm{H}_i)$ and the full ab-initio $\delta_{\mathrm{liq}}(\mathrm{H}_i)$ is presented in Fig. 6. Including into the fit the other hydrogen's covalent or its hydrogen bond length d_2 (see Fig 5) does not reduce $\rho_5^{(\mathrm{fit})}$ significantly.

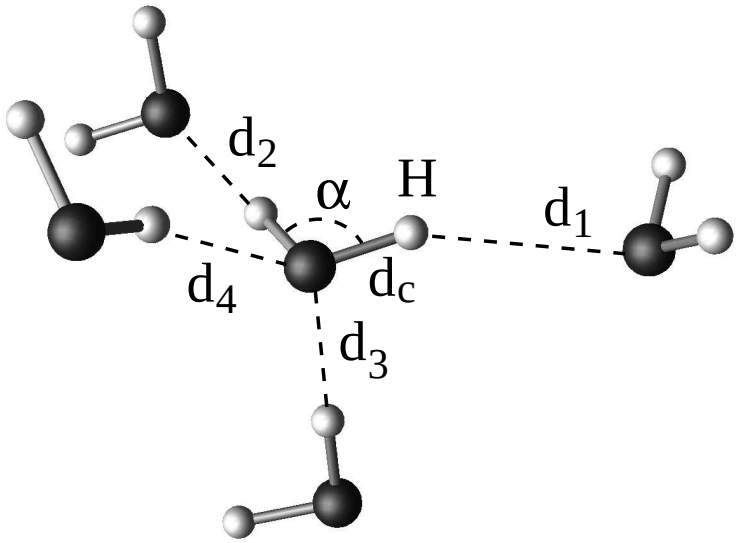

FIG. 5. Geometrical parameters used to calculate $\delta_5^{(\mathrm{fit})}(\mathrm{H}_i)$ in the liquid. Hydrogen atoms are shown in light grey, oxygen atoms in dark grey. The covalent bond length of the hydrogen H under consideration is labeled d_c, its hydrogen bond length d_1, and the secondary hydrogen bond lengths are labeled d_3 and d_4[51]. The other hydrogen's covalent bond length, and the length of its hydrogen bond, d_2, are found to have little influence on the fit, and are therefore not included in Eq. (7).

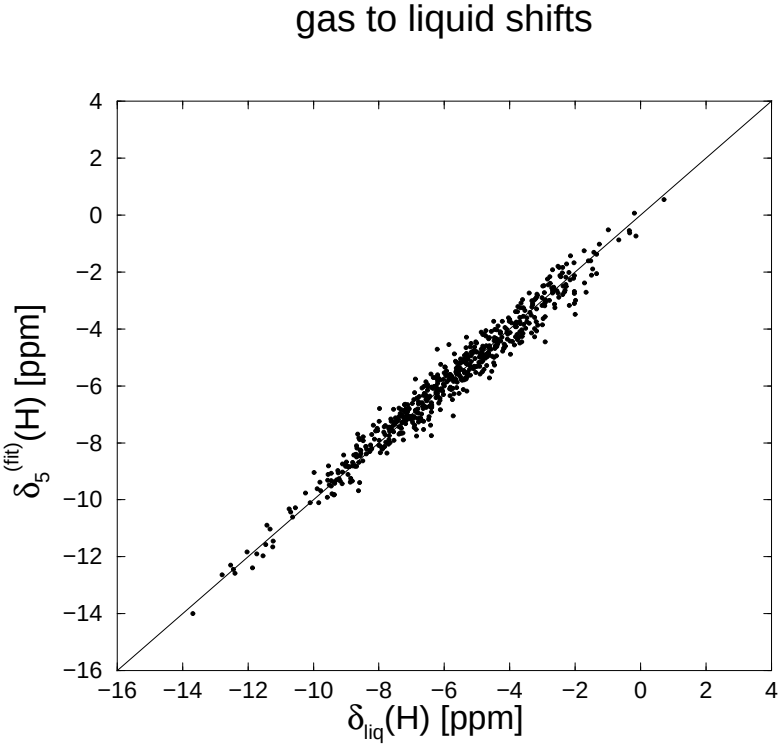

FIG. 6. Isotropic hydrogen chemical shifts $\delta_5^{(\mathrm{fit})}(\mathrm{H}_i)$ of the liquid samples obtained with the fit formula (7), versus the results of the ab initio calculation $\delta_{\mathrm{liq}}(\mathrm{H}_i)$.

To verify the transferability of the fit, we use a snapshot of supercritical water with 32 molecules, generated by an ab-initio MD simulation[52] at a temperature of 730 K and a density of 0.64 g/cm^3, i.e. under conditions which are very far from those used to derive Eq. (7). On this sample, Eq. (7) reproduces the results of the ab-initio calculation with $\rho = 0.61$ ppm. Reoptimising the parameters in Eq. (7) on the snapshot of supercritical water, we obtain a similar value $\rho = 0.55$ ppm, which indicates that the parameters of Eq. (7) are indeed transferable to liquid samples under a wide range of conditions.

The aberration ρ estimates the error in reproducing the shifts $\delta_{\mathrm{liq}}(\mathrm{H}_i)$ of each individual H_i. However, the quantity measured experimentally in the liquid is the average value $\delta_{\mathrm{liq}}(\mathrm{H})$, for which our empirical formula is much more accurate. For each of the nine snapshots of liquid water, and also for the supercritical water sample, the maximum deviation of the average $\delta_5^{(\mathrm{fit})}(\mathrm{H})$ from the full ab initio $\delta_{\mathrm{liq}}(\mathrm{H})$ is less than 0.06ppm[53]. Finally, for the two ice models A and B, Eq. (7) reproduces the average ab-initio results with an error of 0.26ppm and 0.34 ppm, respectively.

If new MD simulations of liquid water are performed in the future, possibly with refined models for the interaction of the water molecules, the average $\delta_{\mathrm{liq}}(\mathrm{H})$ can be easily computed using the fit in Eq. (7), without performing an ab-initio chemical shift calculation. We are confident that the fit is accurate for this purpose, since we have demonstrated the accuracy of (7) for three rather different condensed phases, and forthcoming MD simulations of liquid water are expected to produce molecular geometries similar to the ones of the liquid water samples employed here.

VII. SUSCEPTIBILITIES

As a byproduct of our chemical shift calculations, we obtain the magnetic susceptibilites of condensed water phases. The molar susceptibility χ_M of the isolated reference water molecule is -14.6×10^{-6}cm^3/mol, compared to -13.2×10^{-6}cm^3/mol for liquid water, and -12.8×10^{-6}cm^3/mol or -12.7×10^{-6}cm^3/mol for ice Ih, using model A or model B, respectively. In experiment[54–56], the susceptibilities for liquid ($T = 293$K) and solid ($T = 273$K) water are -12.96×10^{-6}cm^3/mol and -12.65×10^{-6}cm^3/mol, respectively. No experimental results for χ_M in the gas phase could be found in the literature[57].

VIII. CONCLUSION

The electric field does indeed play a major role in explaining the proton condensation shift, since due to the hydrogen bonding network present in the condensed phases, the water molecules surrounding a given proton assume a preferred orientation, which generates a net electric field along the OH bond. However, we also point out shortcomings of a simple electrostatic model, especially when small clusters are used to model configurations with a strong shift. We demonstrate that one can fairly accurately reproduce the full proton shifts in the liquid by using water pentamer clusters, and adding an appropriate electric field to represent the bulk effects. Moreover, we show that it is possible to reproduce the proton chemical shifts in the condensed phases by an empirical function of the local molecular geometry.

In contrast to previous studies on liquid water, which underestimate the proton gas-to-liquid shift[12,14,15] we slightly overestimate it. Most likely, this is due to shortcomings in the molecular geometries on which our calculations rest, and could be a further indicator that the hydrogen bond is too strong in MD simulations performed with the BLYP functional[3]. For ice Ih, our calculated isotropic shift supports one set of experiments[5,6], but is in disagreement with other measurements[7,8]. Combined with more accurate experiments, it could be used to indirectly determine the OH bond length of ice Ih. Finally, our computed magnetic susceptibilities of water and ice are in good agreement with experimental results.

IX. ACKNOWLEDGMENTS

We thank Dr. M. Sprik for making the MD snapshots from Ref. 3 available to us. We also thank Dr. D. R. Hamann for his unpublished results on equillibrium GGA geometries of the water molecule and of ice. B.G.P. acknowledges useful discussions with Dr. M. Mehring. This work was supported by the NSF under Grant No. DMR-9520554, and by the Office of Energy Research, Office of Basic Energy Sciences, Materials Sciences Division of the U.S. Department of Energy under Contract No. DE-AC03-76SF00098. Computer time was provided by the NSF at the National Center for Supercomputing Applications and by the DOE at the Lawrence Berkeley National Laboratory's NERSC center.

[1] L. Pauling, *J. Am. Chem. Soc.* **1935**, *57*, 2680.
[2] A. Katrusiak, *Phys. Rev. Lett.* **1996**, *77*, 4366.
[3] M. Sprik, J. Hutter, and M. Parrinello, *J. Chem. Phys.* **1996**, *105*, 1142.
[4] E. Whalley, *Mol. Phys.* **1974**, *28*, 1105.
[5] D.P. Burum and W.K. Rhim, *J. Chem. Phys.* **1979**, *70*, 3553.
[6] W.K. Rhim, D.P. Burum, and D.D. Elleman, *J. Chem. Phys.* **1979**, *71*, 3139.
[7] A. Pines, D.J. Ruben, S. Vega, and M. Mehring, *Phys. Rev. Lett.* **1976**, *36*, 110.
[8] L.M. Ryan, R.C. Wilson, and B.C. Gerstein, *Chem. Phys. Lett.* **1977**, *52*, 341.
[9] R. Ditchfield, *J. Chem. Phys.* **1976**, *65*, 3123.
[10] J.F. Hinton and D.L. Bennet, *Chem. Phys. Lett.* **1985**, *116*, 292.
[11] R. Höller and H. Lischka, *Chem. Phys. Lett.* **1981**, *84*, 94.
[12] V.G. Malkin, O.L. Malkina, G. Steinebrunner, and H.-P. Huber, *Chem. Eur. J.* **1996**, *2*, 452.
[13] J.F. Hinton, P. Guthrie, P. Pulay, and K. Wolinski, *J. Am. Chem. Soc.* **1992**, *114*, 1604.
[14] D.B. Chesnut and B.E. Rusiloski, *J. Mol. Struct. (Theochem)* **1994**, *314*, 19.
[15] K.V. Mikkelsen, K. Ruud, and T. Helgaker, *Chem. Phys. Lett.* **1996**, *253*, 443.
[16] C. Rohlfing, L.C. Allen, and R. Ditchfield, *Chem. Phys. Lett.* **1982**, *86*, 380.
[17] D.B. Chesnut and B.E. Rusiloski, *J. Phys. Chem.* **1993**, *97*, 2839.
[18] A.C. de Dios, J.G. Pearson, and E. Oldfield, *Science* **1993**, *260*, 1491.
[19] J. Augspurger, J.G. Pearson, E. Oldfield, C.E. Dykstra, K.D. Park, and D. Schwartz, *J. Magn. Reson.* **1992**, *100*, 342.
[20] T.M. Nymand and P.-O. Åstrand, *J. Chem. Phys.* **1997**, *106*, 8332.
[21] F. Mauri, B.G. Pfrommer, and S.G. Louie, *Phys. Rev. Lett.* **1996**, *77*, 5300.
[22] K. Laasonen, M. Sprik, and M. Parrinello, *J. Chem. Phys.* **1993**, *99*, 9080.
[23] W. Kutzelnigg, U. Fleischer, and M. Schindler, The IGLO-Method: Ab-initio Calculation and Interpretation of NMR Chemical Shifts and Magnetic Susceptibilities, In P. Diehl, editor, *NMR basic principles and progress*, volume 23, p. 167. Springer-Verlag, New York, **1990**.
[24] N. Troullier and J.L. Martins, *Phys. Rev. B* **1991**, *43*, 1993.
[25] L. Kleinman and D. M. Bylander, *Phys. Rev. Lett.* **1982**, *48*, 1425.
[26] D.R. Hamann, *Phys. Rev. B* **1997**, *55*, 10157.
[27] D.R. Hamann **1997**, private communication.
[28] J.P. Perdew, K. Burke, and M. Ernzerhof, *Phys. Rev. Lett.* **1996**, *77*, 3865.
[29] When computed with a fully converged basis set, the relaxed molecular geometries are very similar for the PBE and the BLYP functionals, as shown in Ref. 3. Using the PBE relaxed molecule as a reference for the BLYP generated liquid geometries gives rise to an error of only 0.05ppm in the proton shift.
[30] J. D. Augspurger and C.E. Dykstra, *Mol. Phys.* **1993**, *80*, 117.
[31] W. T. Raynes, *Nuclear Magnetic Resonance*, volume 7, The Chemical Society, London, **1977**.
[32] Using the experimental equilibrium geometry[2] of $r_e = 0.9578$Å and $\angle$HOH$= 104.54^o$, we obtain σ_e(H) = 30.4ppm, and $\Delta\sigma_e$(H) = 21.0ppm. Due to its larger absolute value, the oxygen shielding is more sensitive to the reference configuration, and changes by -2.9ppm when going from the GGA-relaxed to the experimental equilibrium geometry.
[33] By performing a force field MD simulation, it has been shown in Ref. 12 that the average gas-phase σ_{gas}(H) deviates only by about 0.1ppm from σ_e(H), and for oxygen, the deviation is on the order of 0.6 ppm.
[34] J. Vaara, J. Lounila, K. Ruud, and T. Helgaker, *J. Chem. Phys.* **1998**, *109*, 8388.
[35] In our calculations for the liquid phase, we automatically include the classical part of the rovibrational corrections. For ice, we assume that they are of similar magnitude as in the gas phase, and can hence be neglected.
[36] I.-M. Chou, J.G. Blank, A.F. Goncharov, H.-K. Mao, and H. Russell, *Science* **1998**, *281*, 809.
[37] C. Lobban, J.L. Finney, and W.F. Kuhs, *Nature* **1998**, *391*, 268.
[38] W.F. Kuhs and M.S. Lehmann, *Water Sci. Rev.* **1986**, *2*, 1.
[39] J.C. Hindman, *J. Chem. Phys.* **1966**, *44*, 4582.
[40] M. Mehring **1997**, private communication.
[41] S.W. Peterson and H.A. Levy, *Acta crystallogr.* **1953**, *10*, 70.
[42] J.S. Chamberlain, F.H Moore, and N.H. Fletcher, Neutron-diffraction study of H_2O ice at 77K, In E. Whalley, S.J. Jones, and L.W. Gold, editors, *Symposium on the Physics and Chemistry of Ice*, p. 283, Ottawa, **1973**, Royal Soc. Canada.
[43] R. Car and M. Parrinello, *Phys. Rev. Lett.* **1985**, *55*, 2471.
[44] V.G. Malkin, O.L. Malkina, M.E. Casida, and D.R. Salahub, *J. Am. Chem. Soc.* **1994**, *116*, 5393.
[45] G.C. Lie and E. Clementi, *Phys. Rev. A* **1986**, *33*, 2679.
[46] A.E. Florin and M. Alei, *J. Chem. Phys.* **1967**, *47*, 4268.

[47] I.M. Svishchev and P.G. Kusalik, *J. Am. Chem. Soc.* **1993**, *115*, 8270.
[48] J. Gauss, *Chem. Phys. Lett.* **1994**, *229*, 198.
[49] J. Gauss, *Ber. Bunsenges. Phys. Chem.* **1995**, *99*, 1001.
[50] A. Rizzo, T. Helgaker, K. Ruud, A. Barszczewicz, M. Jaszunski, and P. Jorgensen, *J. Chem. Phys.* **1995**, *102*, 8953.
[51] The algorithm for computing the distances is as follows: d_1 is the shortest intermolecular H$\cdots$O distance; d_2 is the shortest intermolecular distance from the second hydrogen to an oxygen molecule that is distinct from that used to compute d_1; d_3 is the shortest intermolecular distance from the central molecule's oxygen to a H belonging to a molecule distinct from those used to compute d_1 and d_2. Finally, d_4 is computed like d_3, just that the H atom must belong to a molecule different from the one used to compute d_1, d_2, and d_3.
[52] E.S. Fois, M. Sprik, and M. Parrinello, *Chem. Phys. Lett.* **1994**, *223*, 411.
[53] Notice that the chemical shift of the central H in an isolated pentamer changes by ~ 1 ppm when the pentamer is embedded in the liquid. Therefore, the fit performed of the liquid samples is not transferable to isolated pentamer clusters. However, the quality of the fit on liquid water, and its transferability to ice and supercritical water indicate that in the condensed phases, the effect of the molecules beyond the first coordination shell is well described by a function of the pentamer geometry only.
[54] B. Cabrera and H. Fahlenbrach, *Z. Physik* **1933**, *82*, 759.
[55] B. Cabrera and H. Fahlenbrach, *Naturwissenschaften* **1934**, *22*, 417.
[56] R.C. Weast, *CRC Handbook of Chemistry and Physics*, The Chemical Rubber Co, Cleveland, Ohio, 53rd edition, **1972**.
[57] Ref. 56 quotes a value of $\chi_M = -13.1 \times 10^{-6}\mathrm{cm}^3/\mathrm{mol}$ for water in the gas phase. We do not trust this number, since it is claimed to be taken from Refs. 54 and 55, which, upon closer examination, *do not* report measurements on water in the gas phase.